THE ARRAY SCANNING METHOD AND APPLYING IT TO DETERMINE THE IMPEDANCE OF LINEAR ANTENNAS IN A LOSSY HALF SPACE

G.A. Burrell and B.A. Munk

The Ohio State University

ElectroScience Laboratory

Department of Electrical Engineering
Columbus, Ohio 43212

Technical Report 4460-1

October 1976

Contract DAAG53-76-C-0179

Department of the Army
US Army Mobility Equipment Research & Development Command
Ft. Belvoir, Virginia 22060

NOTICES

When Government drawings, specifications, or other data are used for any purpose other than in connection with a definitely related Government procurement operation, the United States Government thereby incurs no responsibility nor any obligation whatsoever, and the fact that the Government may have formulated, furnished, or in any way supplied the said drawings, specifications, or other data, is not to be regarded by implication or otherwise as in any manner licensing the holder or any other person or corporation, or conveying any rights or permission to manufacture, use, or sell any patented invention that may in any way be related thereto.

UNCLASSIFIED

SECURITY CLASSIFICATION OF THIS PAGE *(When Data Entered)*

REPORT DOCUMENTATION PAGE

READ INSTRUCTIONS BEFORE COMPLETING FORM

1. REPORT NUMBER	2. GOVT ACCESSION NO. AD-A044 364 / 3. RECIPIENT'S CATALOG NUMBER
4. TITLE *(and Subtitle)* THE ARRAY SCANNING METHOD AND APPLYING IT TO DETERMINE THE IMPEDANCE OF LINEAR ANTENNAS IN A LOSSY HALF SPACE	5. TYPE OF REPORT & PERIOD COVERED: Technical Report 6. PERFORMING ORG. REPORT NUMBER: ESL 4460-1
7. AUTHOR(s) G.A. Burrell, B.A. Munk	8. CONTRACT OR GRANT NUMBER(s): Contract DAAG53-76-C-0179
9. PERFORMING ORGANIZATION NAME AND ADDRESS The Ohio State University ElectroScience Laboratory, Department of Electrical Engineering, Columbus, Ohio 43212	10. PROGRAM ELEMENT, PROJECT, TASK AREA & WORK UNIT NUMBERS
11. CONTROLLING OFFICE NAME AND ADDRESS Department of the Army, US Army Mobility Equipment Research & Development Command, Ft. Belvoir, Virginia 22060	12. REPORT DATE: October 1976 13. NUMBER OF PAGES: 34
14. MONITORING AGENCY NAME & ADDRESS *(If different from Controlling Office)*	15. SECURITY CLASS. *(of this report)*: Unclassified 15a. DECLASSIFICATION/DOWNGRADING SCHEDULE
16. DISTRIBUTION STATEMENT *(of this Report)*	
17. DISTRIBUTION STATEMENT *(of the abstract entered in Block 20, If different from Report)*	
18. SUPPLEMENTARY NOTES	

19. KEY WORDS *(Continue on reverse side if necessary and identify by block number)*

Arrays	Moment Method
Impedance	Underground Radar
Half Space	Numerical Results
Dipoles	Array Scanning Method
Sommerfeld	Linear Antennas

20. ABSTRACT *(Continue on reverse side if necessary and identify by block number)*

This report presents a simple plane wave expansion for the mutual impedance between two parallel sinusoidal dipoles. Complex plane wave reflection coefficients are then introduced to account for a parallel plane interface. The mutual impedance is inferred from a previously reported solution for an infinite array[3]. This technique is called the Array Scanning Method (ASM) and has a clear physical interpretation which greatly facilitates its use. It can be applied to moment method solutions of wire antennas using Galerkins method with a piecewise sinusoidal expansion for the current. Numerical

DD FORM 1 JAN 73 1473 EDITION OF 1 NOV 65 IS OBSOLETE

UNCLASSIFIED

SECURITY CLASSIFICATION OF THIS PAGE *(When Data Entered)*

evaluation is straightforward when the dipole is in the lossy half-space, and the utility of the method is demonstrated by the presentation of results for the input impedance of dipoles in a variety of half space environments. Computer time is proportional to d^{+1}, where d is the distance of the dipole from the half space. For conducting media and low frequencies an approximation is made to reduce computation time. The moment method solution of a dipole buried at depth as small as 1/150,000 wavelength in the earth is presented.

FOREWORD

This report was initiated under a Post Doctoral Grant with the Ohio State University and completed under Contract DAAG53-76-C-179 for Department of the Army, US Army Mobility Equipment Research and Development Command, Ft. Belvoir, Virginia 22060 by the Ohio State University Research Foundation, Columbus, Ohio 43212.

Professor Jack H. Richmond is thanked for providing the induced EMF subroutine SPARG.

One of us (G.A.B.) is grateful for the assistance provided by a Fulbright travel grant from the New Zealand-United States Educational Foundation and an Ohio State University Post Doctoral Fellowship.

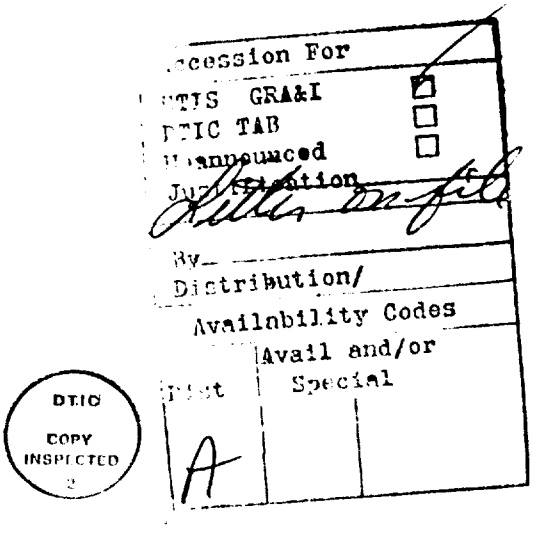

TABLE OF CONTENTS

I. INTRODUCTION

Calculation of the input impedance of a dipole antenna located electrically close to a plane dielectric interface has traditionally involved a Sommerfeld integral formulation. This is well known to be a time consuming and difficult computational task. A good bibliography can be found in a book by Banos[1]. A disadvantage of the Sommerfeld formulation is that the mathematical manipulations involved in obtaining a better approximation or a better integration path seldom have a clear physical explanation. This means that it is often difficult to decide what action to take to facilitate the computation. Sommerfeld solutions for finite length antennas are difficult to program successfully and the resulting program is usually lengthy.

This report presents a simple yet exact formulation for the mutual impedance between two sinusoidal dipole antennas in the presence of a half space. This formula can be simply evaluated numerically when the dipoles are immersed in a lossy medium, and can be used in a moment method solution using sinusoidal bases and Galerkins method[2]. The resulting program is relatively compact. The mutual impedance is inferred (by the Array Scanning Method) from a convenient formula for the infinite array impedance developed by Munk, et al[3] which contains a sum of plane waves. The half space is accounted for by including a plane wave reflection coefficient for each plane wave. The advantages of this formulation are that it is exact, it is simple to program, and it has a clear physical interpretation.

The Array Scanning Method formulation is presented in Section II. Section III discusses the result. The utility of the method is demonstrated in Section IV by the presentation of numerical results of the input impedance of dipoles in lossy half spaces. Several different cases are presented because there are few results of half space calculations contained in the literature. In Section V an approximation is made for low frequencies and conducting media which results in a considerable saving in computer time. As an example a moment method solution for the input impedance for a dipole buried in the earth is presented. The change in the current distribution as the dipole approaches to within $\lambda/150{,}000$ of the surface is shown.

II. THE MUTUAL IMPEDANCE BETWEEN TWO SINUSOIDAL DIPOLES IN TERMS OF PLANE WAVES

Munk, et al[3] have developed a convenient formulation for the free space mutual impedance between a reference dipole located parallel to an infinite two dimensional plane array of parallel sinusoidal dipoles. The formula converges much faster on a computer than does the method in which the mutual impedances of the individual elements are summed. Referring to Fig. 1, the mutual impedance between the reference dipole and the array when both are in a general medium of propagation constant

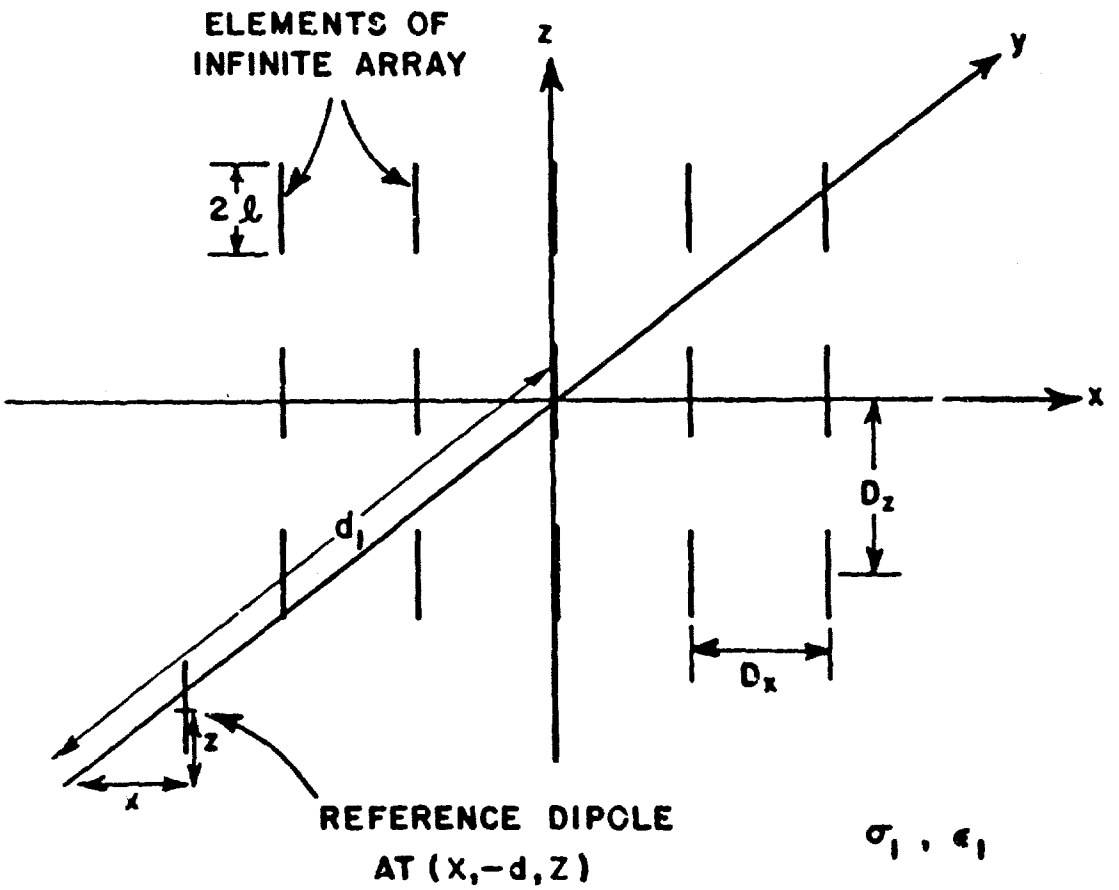

Fig. 1. Geometry of reference dipole and infinite array.

$\gamma = \alpha + j\beta$, and all elements have a sinusoidal distribution of the Floquet type is

$$(1) \qquad Z_M^a = \frac{2n}{D_z D_x} \sum_{n_0=-\infty}^{\infty} p^2(\theta)\, e^{j\beta Z s_\theta} \sum_{k_0=-\infty}^{\infty} e^{j\beta X s_\phi}\, \frac{e^{-\gamma d_1 c_y}}{\gamma c_y}$$

where the superscript denotes an array impedance, and

$$(2) \qquad c_y = \sqrt{1 + \frac{\beta^2}{\gamma^2}\,(s_\theta^2 + s_\phi^2)}$$

is a direction cosine. The other directions cosines c_x, c_z are given in Eqs. (47) and (48) of Appendix A. The other terms are

$$(3) \qquad P^2(\theta) = \frac{\gamma[\cos\beta\ell s_\theta - \cosh\gamma\ell]^2}{[\beta^2 s_\theta^2 + \gamma^2]\sinh^2\gamma\ell}$$

$$(4) \qquad s_\theta = \sin\theta + \frac{n_o\lambda}{D_z}$$

$$(5) \qquad s_\phi = \sin\phi + \frac{k_o\lambda}{D_x}$$

$\eta = \sqrt{\mu/\epsilon}$ is the characteristic impedance of the medium, and θ and ϕ are the phase differences between the current on adjacent array elements in the z and x directions respectively. The significance of the summation indices will be clarified in the following section.

By applying simple Fourier theory during the derivation of Eq. (1), we instead obtain an expression for the mutual impedance between the reference dipole and a single array element centered at the origin of the coordinate system shown in Fig. 1:

$$(6) \qquad Z_M = \int_{-\pi/\beta D_z}^{\pi/\beta D_z} \int_{-\pi/\beta D_x}^{\pi/\beta D_x} Z_M^a \, d(\sin\phi)d(\sin\theta) \quad .$$

The details of the derivation are given in Appendix A. The derivation of Eq. (1) is implicit in Appendix A.

III. INTERPRETATION OF THE RESULT

Notice that in Eq. (6) that the integration is done with respect to the variables $\sin\phi$ and $\sin\theta$ which by Eqs. (2), (47) and (48) control the direction of propagation of the plane waves emitted by the infinite array (changing the phase of the current on the elements to control the direction of radiation is called scanning). Therefore implicit in Eq. (6) is a plane wave expansion of the spherical wave field emitted by a single dipole, and the technique is called the Array Scanning Method (ASM). The advantage gained in this approach is that a clear physical interpretation is obtained, viz. that the plane waves are emitted by an infinite array in which the wanted antenna is a member element.

It is instructive to examine the behaviour of the direction cosine c_y. Figure 2 shows c_y for an array having a spacing $D_z = 3.5\lambda$ with all elements driven with equal phase ($\sin\theta = \sin\phi = 0$), both for free space,

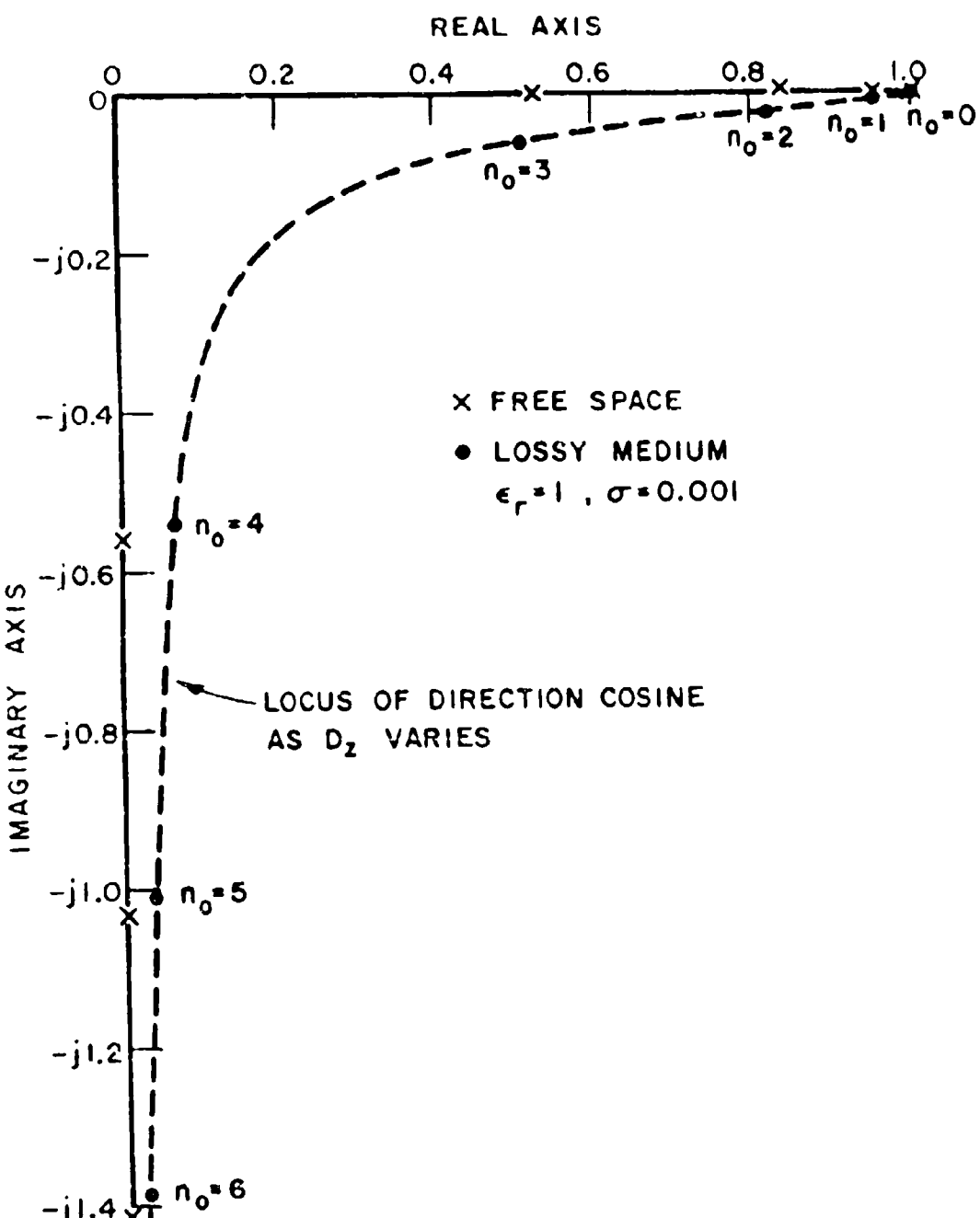

Fig. 2. Example of direction cosine c_y for an array in free space and in a lossy medium. For the array, D_z=3.5λ, sinθ= sinφ= K_0=0. The frequency is 300 MHz.

and for a lossy medium of constitutive parameters ϵ_r=1, σ = .001 mhos/meter. The values are plotted for $k_0 = 0$.

For no loss, when $n_0 \leq 3$, c_y is real. This means that the array emits propagating waves in directions specified by the direction cosines c_x, c_y, c_z. Since $k_0 = 0$, $c_x = 0$ so that the direction of radiation is always in the y-z plane. The radiation associated with $n_0 = 0$ occurs in a direction specified by the element phases, $\sin\theta$ and $\sin\phi$. If $\sin\theta = \sin\phi = 0$, the array radiates broadside. This is the principal direction or main lobe. For $n_0 = 1$, 2 or 3, the radiation occurs in other directions; these are the grating lobes.

When $n_0 > 3$, c_y becomes imaginary, so that the plane waves in Eq. (1) are non-propagating or evanescent waves. The imaginary direction cosines specify the directions of propagation into imaginary space. The evanescent waves decay rapidly as the spacing d_1 from the array increases, and as n_0 increases. It is this rapid decay which makes Eq. (1) converge rapidly.

When the medium is lossy, c_y is complex and lies on the curve shown in Fig. 2. Thus the propagating waves are attenuated, and there are no purely evanescent waves for an infinite array in a lossy medium. However, when $n_0 > 3$ the attenuation factor becomes so large that in practice the waves decay in the same way as in the lossless case.

In Eq. (6) it is convenient to choose the array spacings $D_x = D_z = 0.5\lambda$, so that the limits of integration become -1 and +1. Figure 3 depicts the region of integration for the half-wavelength spaced array in free space. For free space this diagram is known as the direction cosine plane[4]. It is seen that Eq. (6) corresponds to scanning the principal beam of the array over a cell consisting of all real space (that within the circle) and part of imaginary space. Further, because of the form of the summation in Eq. (1) the integration is effectively being carried out over all space (in Fig. 3, as the main lobe scans the pictured square cell, the evanescent modes are scanning an infinite number of identical square cells covering all space). Notice that when $c_x^2 + c_z^2 > 1$, c_y is imaginary and the array does not radiate. Under this condition the mutual impedance is purely reactive. Notice also that when $c_x^2 + c_z^2 = 1$, $c_y = 0$ and the mutual impedance is infinite. It is this "infinite ridge" on the real-imaginary space boundary which makes Eq. (6) difficult to evaluate numerically for a free space medium. However numerical experiments show that the integral does converge when the "pole" is approached. This verifies a conclusion reached on purely physical grounds: if the integral did not converge the mutual impedance between two dipoles would be infinite regardless of spacing. However when the medium is lossy, c_y is never zero, and it is then straightforward to evaluate Eq. (6) numerically. Figure 4 gives an example of the variation of the mutual impedance between the reference element and an array in a lossy medium as the scan angles θ and ϕ are varied. The resistance and reactance (shown separately in Fig. 4) are plotted for the first quadrant of the square cell depicted in Fig. 3. The position of the ridge is shown clearly.

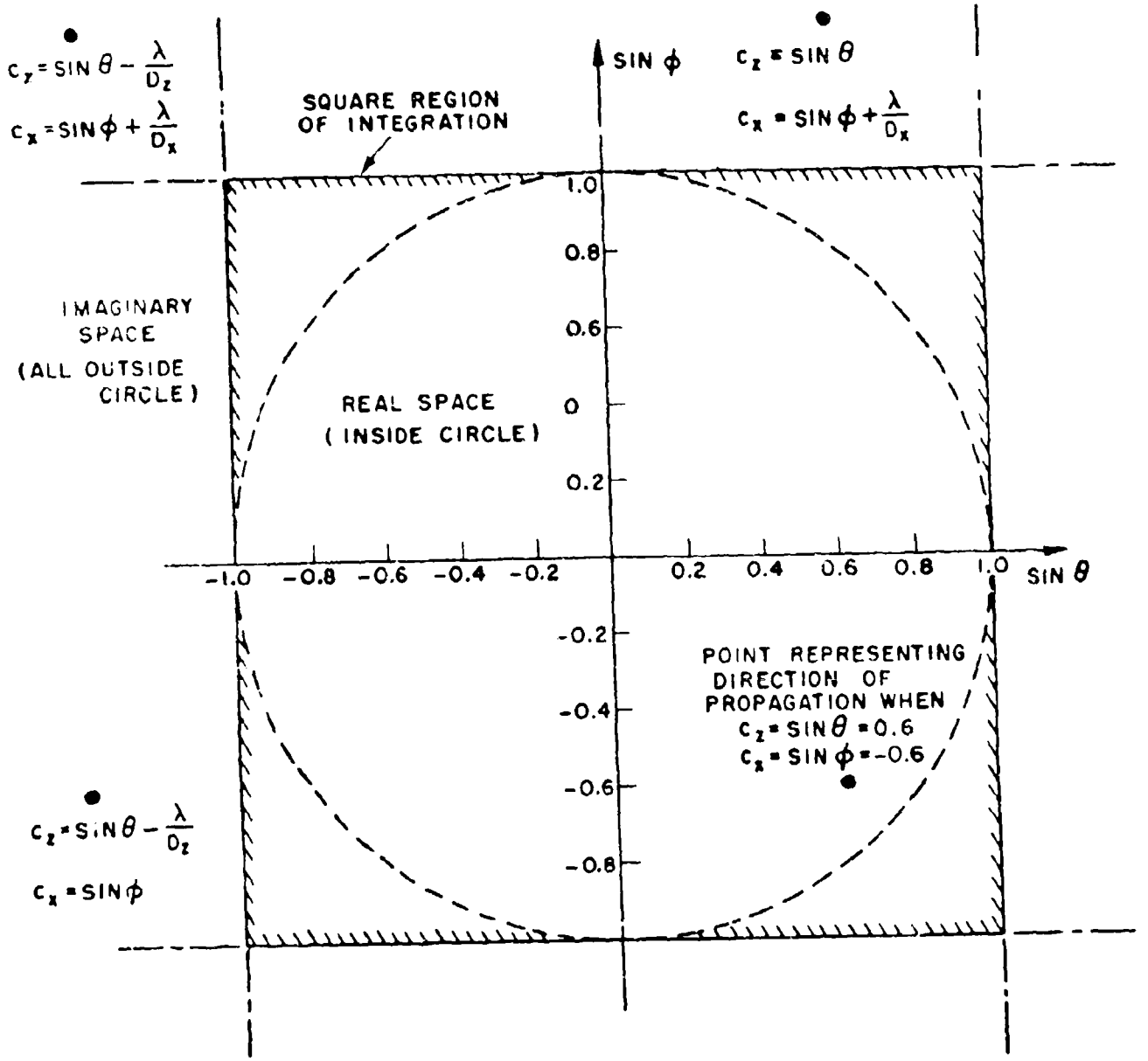

Fig. 3. Depicting the region of integration for half wavelength spaced array in free space.

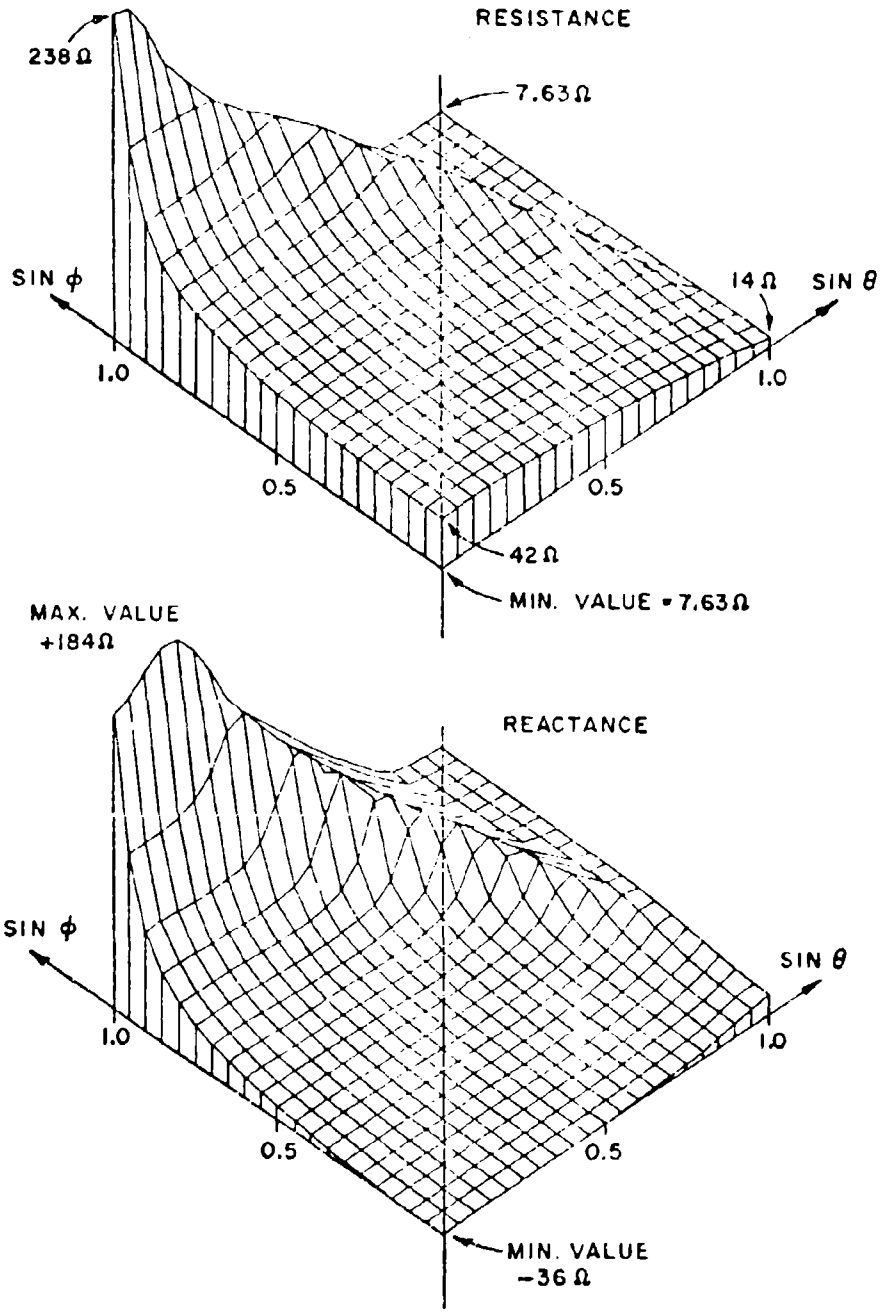

Fig. 4. Variation of mutual impedance with scan angles for half wavelength spaced array of 0.4 m dipoles at 300 MHz. The reference dipole was 0.05 m from the centre element, and the constitutive parameters of the medium were ε_r=1, σ=0.001 mhos/m.

IV. THE IMPEDANCE OF DIPOLES IN A LOSSY HALF-SPACE

When the separation d of the reference dipole and the array is set equal to the dipole radius a we obtain the self impedance[5]. Next, the mutual impedance of an image antenna in a plane interface can be computed simply by including a plane wave reflection coefficient for each plane wave in Eq. (1). The input impedance of a sinusoidal dipole parallel to a plane interface is then given by

$$Z_{in} = Z_M(a) + r_{n_o,k_o}\, Z_M(2d) \qquad (7)$$

The geometry is shown in Fig. 5. r_{n_o,k_o} is an effective plane wave reflection coefficient (i.e., including dipole polarization decoupling and surface waves when they exist) for an array of z directed dipoles parallel to a plane interface. It is given by [3]

$$r_{n_o,k_o} = \frac{1}{(1-c_z)^2(1-c_y^2)} \left[c_y^2 c_z^2 \frac{\sqrt{\left(\frac{\epsilon_2'}{\epsilon'}\right) - (1 - c_y^2)} - \left(\frac{\epsilon_2'}{\epsilon'}\right) c_y}{\sqrt{\left(\frac{\epsilon_2'}{\epsilon'}\right) - (1 - c_y^2)} + \left(\frac{\epsilon_2'}{\epsilon'}\right) c_y} + c_x^2 \frac{c_y - \sqrt{\frac{\epsilon_2'}{\epsilon'} - (1 - c_y^2)}}{c_y + \sqrt{\frac{\epsilon_2'}{\epsilon'} - (1 - c_y^2)}} \right] \qquad (8)$$

where c_x, c_y and c_z are the direction cosines of the incident plane wave. ϵ' and ϵ_2' are the complex dielectric constants of the medium containing the antenna and the half space respectively, and are given by

$$\epsilon' = \epsilon - j\sigma/\omega \qquad (9)$$

$$\epsilon_2' = \epsilon_2 - j\sigma_2/\omega \qquad (10)$$

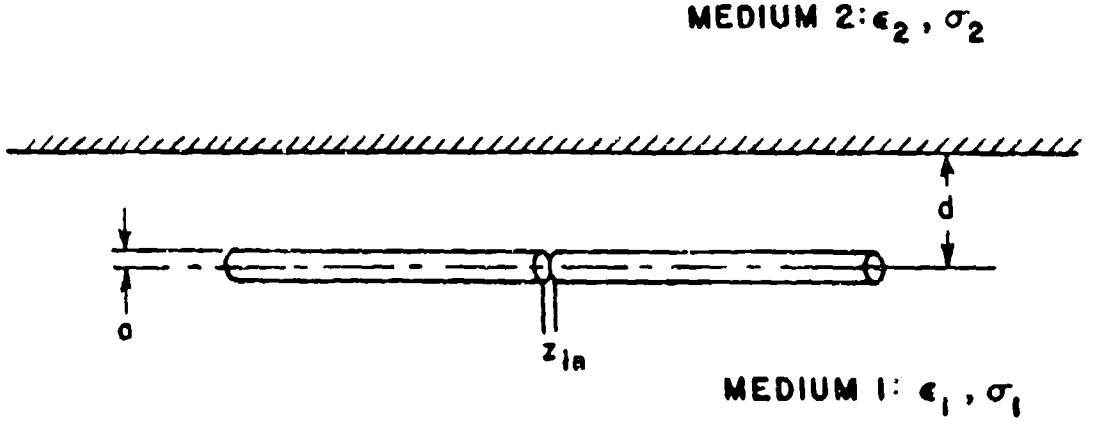

Fig. 5. Geometry of dipole parallel to a plane interface.

The model of Eq. (7) obtained using a sinusoidal dipole represents a two segment moment method solution using the sinusoidal reaction technique [2]. Hence Eq. (7) can be used in multisegment moment method solutions using piecewise sinusoidal expansion dipoles and Galerkins method.

To demonstrate the utility of the ASM several examples of the input impedance of a 0.1 m long, 0.001 m radius sinusoidal dipole parallel to plane interfaces have been computed at a frequency of 300 MHz. All media are lossy dielectrics ($\beta > \alpha$) at 300 MHz. In computing these results the displacements X and Z were zero, and advantage was taken of the symmetry of Eq. (6) about the $\sin\theta$ and $\sin\phi$ axes, i.e., integration need only be done for positive $\sin\theta$ and $\sin\phi$. The integration was done by the trapezoidal rule, and the required number of integration steps N along each axis, and the required convergence accuracy for the series were determined by numerical experiment. This involved comparing the mutual impedance computed using Eq. (6) to those computed by the induced emf method using closed form expressions for the exponential integrals.

For a frequency of 300 MHz, the following values given in Table I consistently gave accuracies better than 2%. A reduction in the convergence accuracy to 10^{-3} gave an accuracy of about 5%.

TABLE I

SUGGESTED VALUES FOR N AND CONVERGENCE ACCURACY
AT 300 MHz. VALUES ARE FOR TRAPEZOIDAL INTEGRATION

σ	d	N	Convergence accuracy
.001	$\leq 0.2\lambda$	15	10^{-4}
.01	$> 0.2\lambda$ $\leq 0.2\lambda$	15 10	10^{-4} 10^{-4}
0.1	all d	10	10^{-4}
1.0	all d	6	10^{-4}

Since Eq. (1) converges more slowly as the distance d becomes small, the computing efficiency was further improved by computing the self impedance of the dipole (the first term in Eq. (7)) by the induced emf method. The plane wave expansion was used only to calculate the mutual impedance of the image in the interface.

Figures 6 and 7 show the input impedance of the dipole when it approaches an interface which has a different permittivity. Results are presented for the dipole on both sides of the interface. Figure 6 shows that when the conductivity σ = .001 mhos/m there is little change in the input resistance, but the reactance is lower when the dipole is in the medium of higher permittivity. This occurs because the shorter wavelength in medium 1 means that the dipole is electrically longer and therefore is nearer to resonance. The smooth reactance change as the dipole approaches the interface occurs because of the influence of the nearby half-space on the wavelength as the dipole approaches the interface. When the conductivity of both media is increased to 0.01 mhos/m, we observe in Fig. 7 that the input resistance has increased significantly. This occurs because the characteristic impedance η for the lossier medium has a larger imaginary part. Thus the evanescent modes summed in Eq. (1), which affect only the reactance when the medium is lossless (η real), now contribute significantly to the resistance because of the complex η multiplier in Eq. (1).

Figures 8-10 show the input impedance when the dipole approaches the interface of a medium of different conductivity. When the conductivity is low, as in Fig. 8, there is little change in the wavelength and in the real part of η, so that there is little change in the dipole reactance. The relatively large change in the imaginary part of η causes the observed change in the input resistance. In Fig. 9, when the conductivity is increased so that there is a significant wavelength change

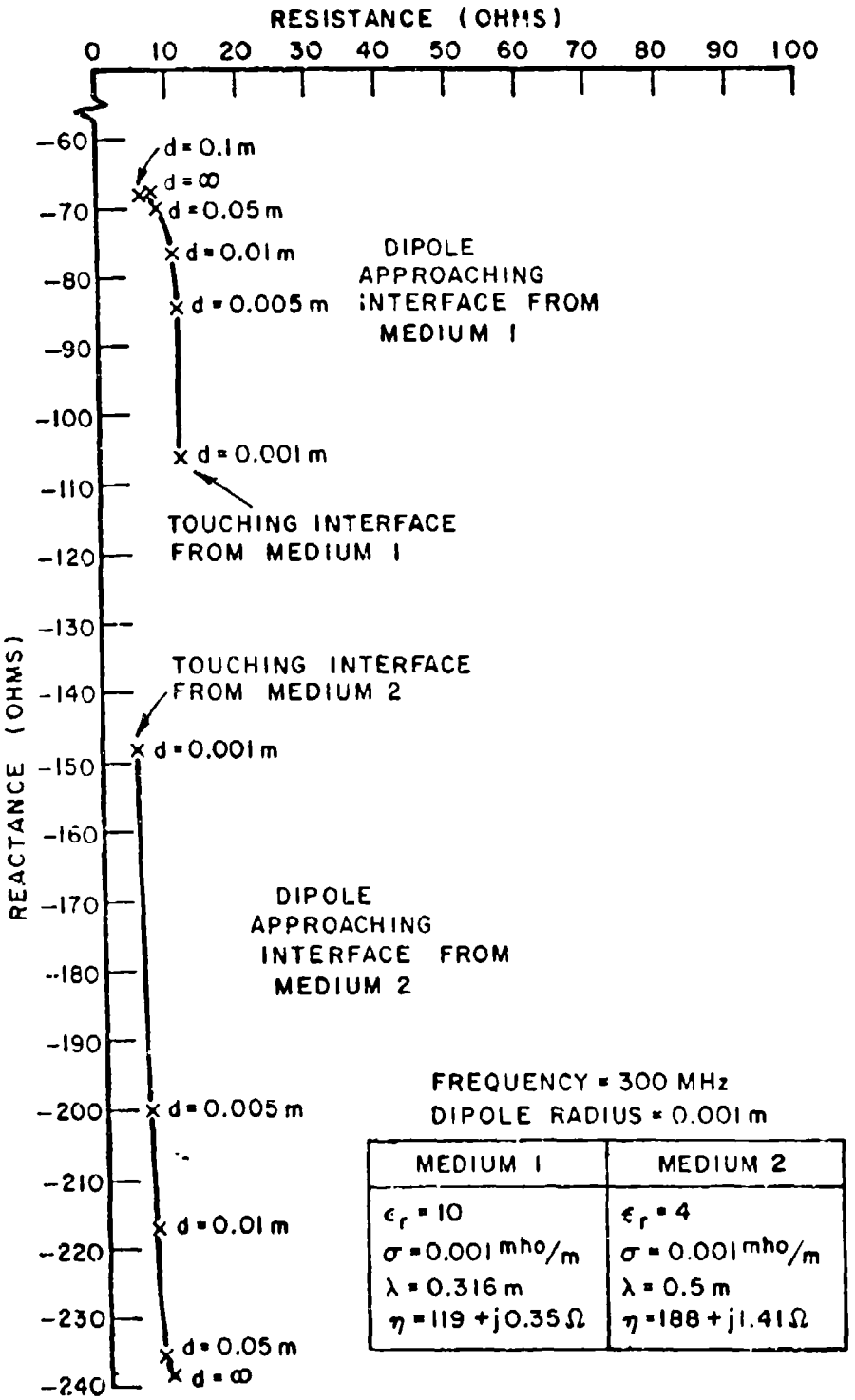

MEDIUM 1	MEDIUM 2
$\epsilon_r = 10$	$\epsilon_r = 4$
$\sigma = 0.001$ mho/m	$\sigma = 0.001$ mho/m
$\lambda = 0.316$ m	$\lambda = 0.5$ m
$\eta = 119 + j0.35\,\Omega$	$\eta = 188 + j1.41\,\Omega$

Fig. 6. Input impedance of 0.1m sinusoidal dipole in media of conductivity 0.001, and parallel to plane interface of different permittivity.

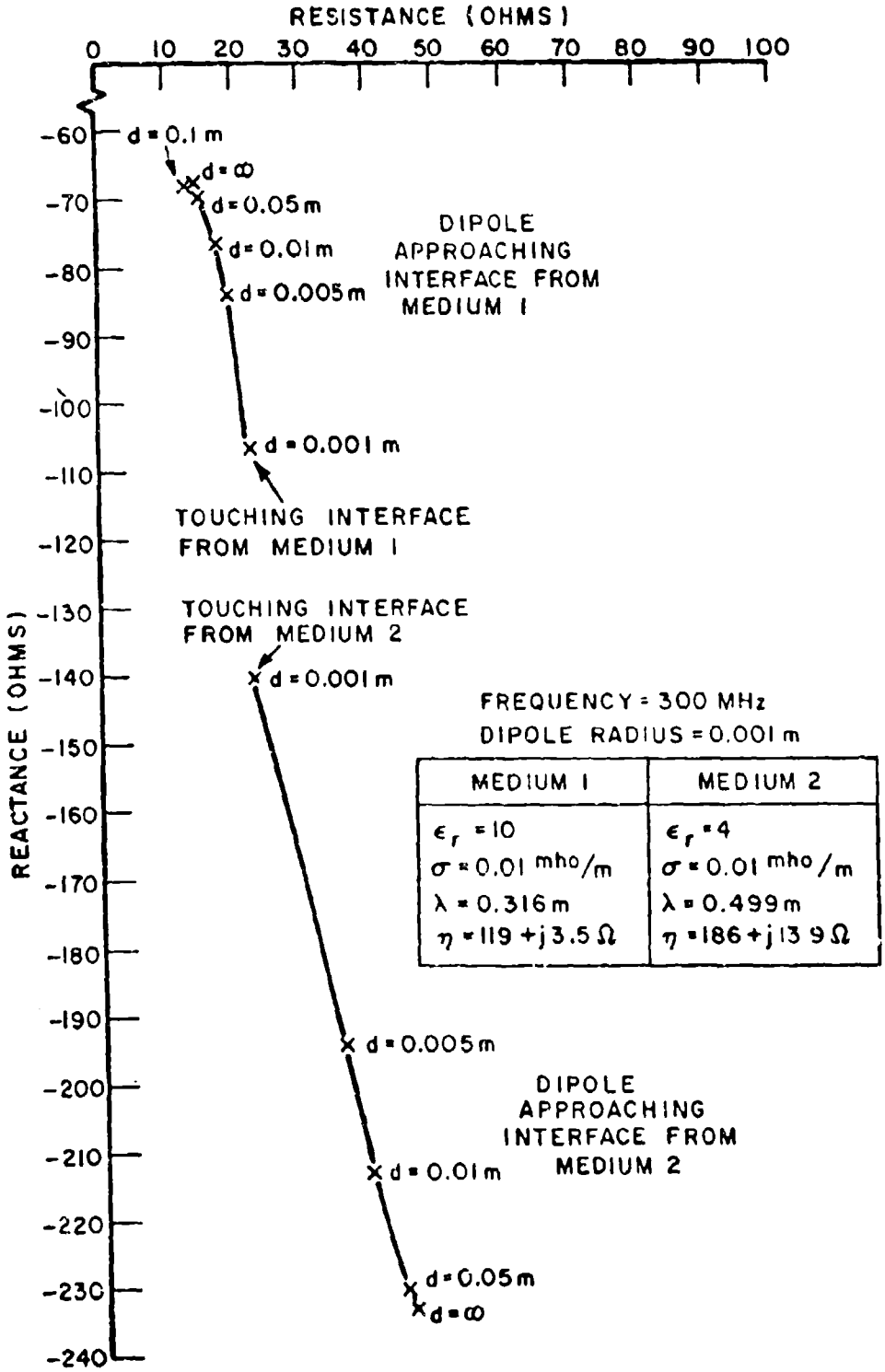

Fig. 7. Input impedance of 0.1m sinusoidal dipole in media of conductivity 0.01 , and parallel to plane interface of different permittivity.

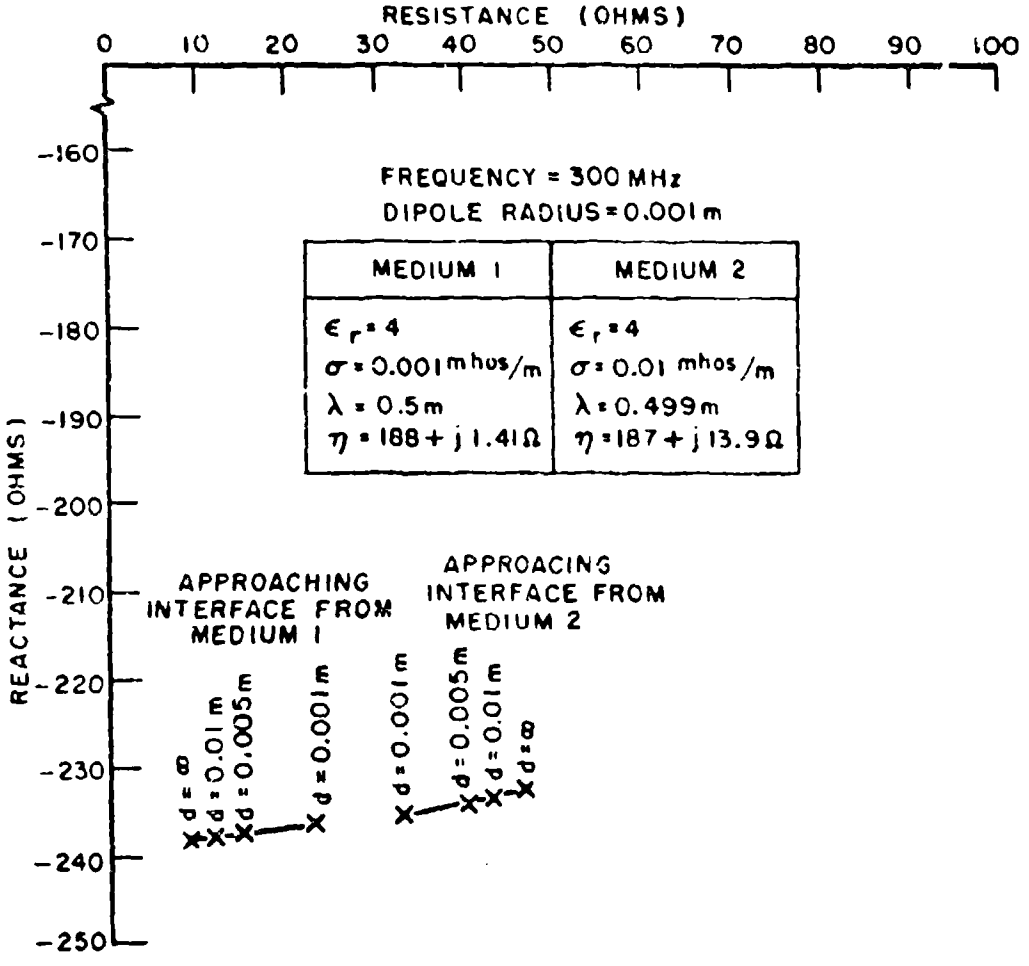

Fig. 8. Input impedance of 0.1m sinusoidal dipole in media of relative permittivity 4, and parallel to plane interface of different conductivity.

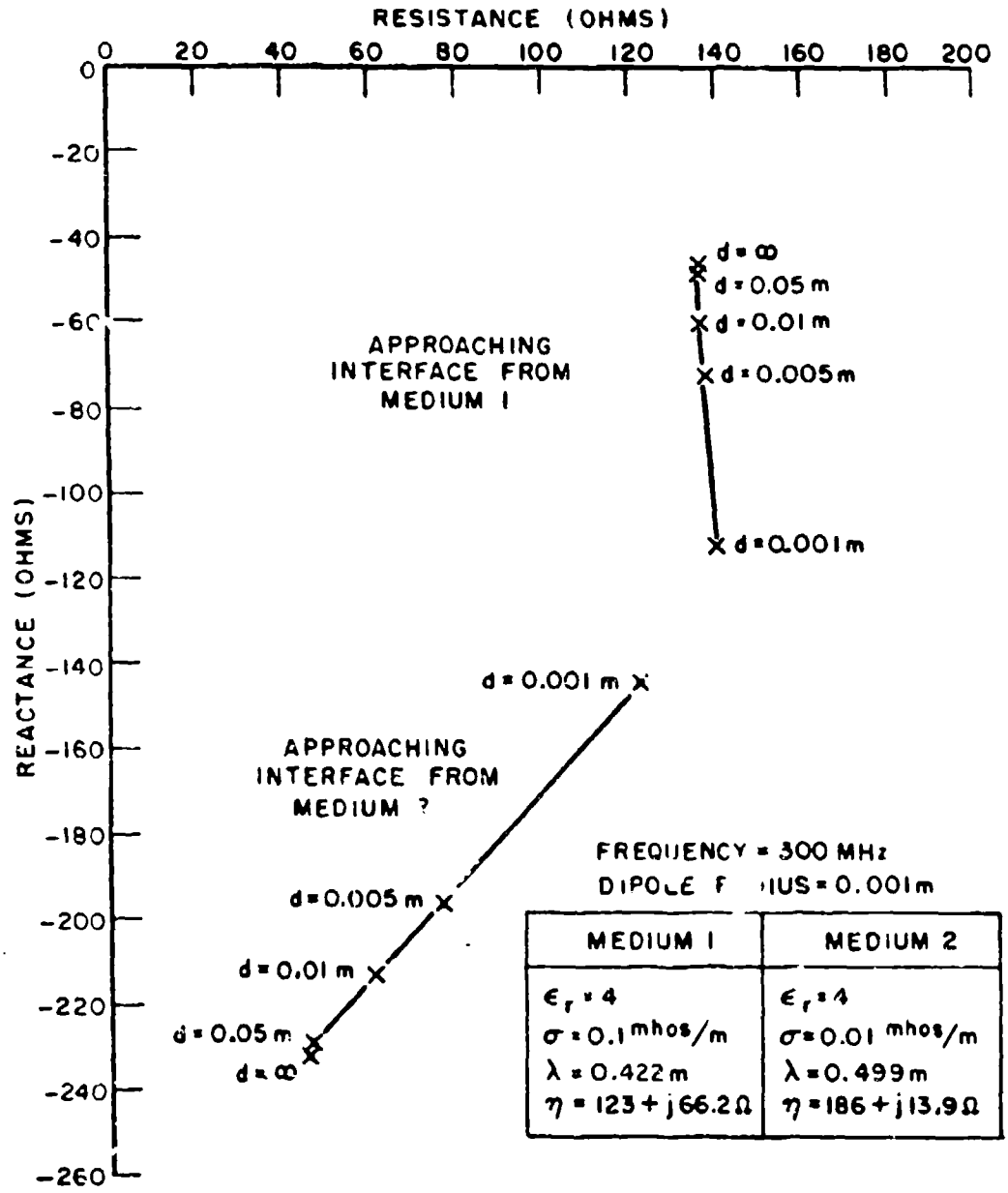

Fig. 9. Input impedance of 0.1m sinusoidal dipole in media of relative permittivity 4, and parallel to plane interface of different conductivity.

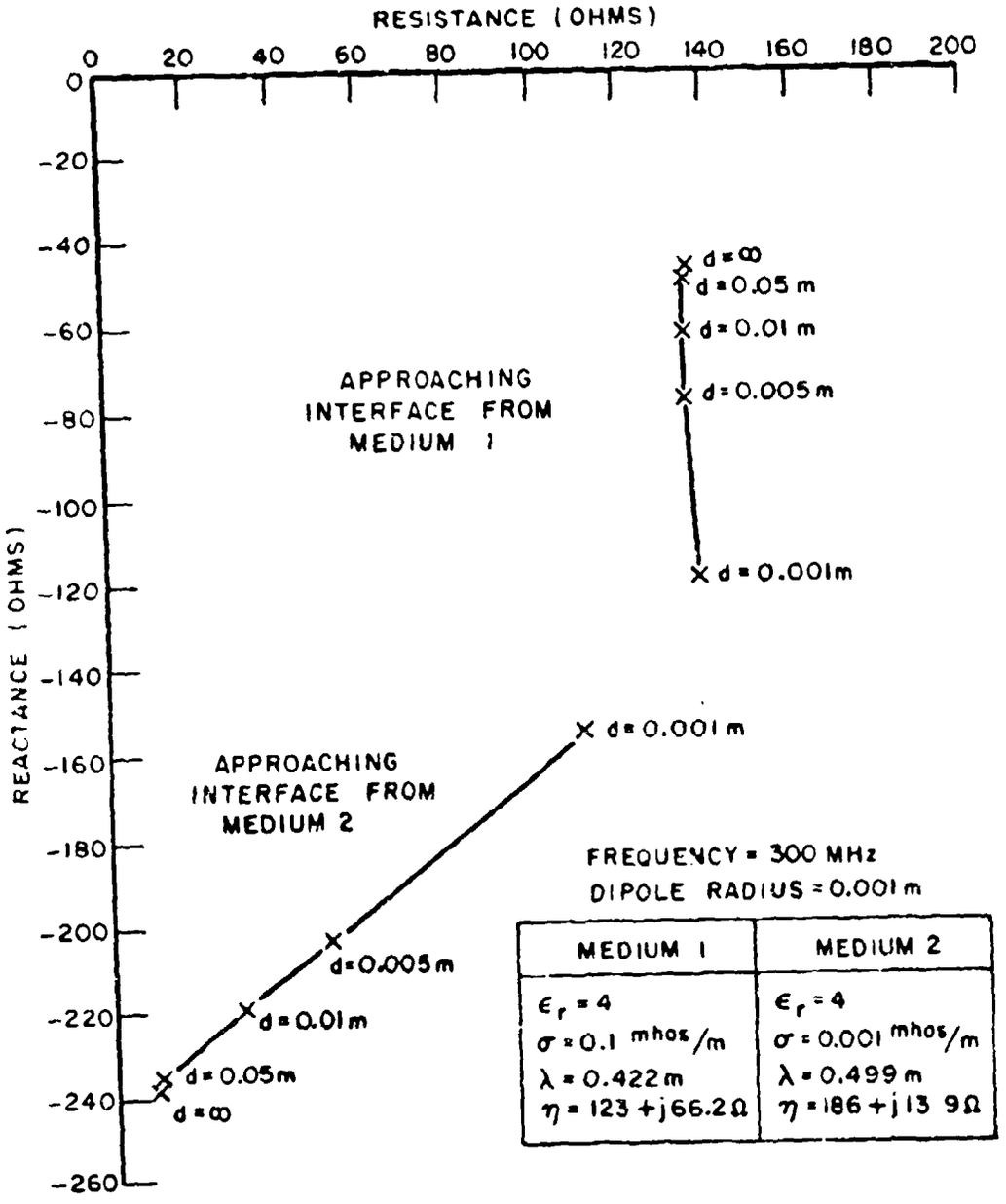

Fig. 10. Input impedance of 0.1m sinuscidal dipole in media of relative permittivity 4, and parallel to plane interface of different conductivity.

between the media, a significant reactance change is observed. An interesting observation is that practically all the resistance change occurs when the dipole is in the medium with the lowest conductivity. This indicates that the medium of lowest characteristic impedance absorbs most of the power supplied to the dipole when the dipole is close to the interface but is located in an adjacent medium of higher characteristic impedance. This effect is even more pronounced in Fig. 10 where the two media differ in conductivity by two orders of magnitude.

Because of their simplicity dipole antennas make good subterranean radar antennas[6]. Consequently the characteristics of dipoles buried in the ground near the earth-air interface are of interest. Figure 11 shows how the input impedance of a 0.001 m radius, 0.1 m long dipole varies with different burial depths in earth having constitutive parameters $\varepsilon_r = 4$, $\sigma = .01$ mhos/m. Three curves are shown. One is a direct application of Eq. (7). For comparison results obtained from a four segment moment method using sinusoidal bases and Galerkins method with Eq. (7) to obtain the impedance matrix elements are also presented. Note that for the electrically short dipole considered good accuracy is obtained with a two segment solution. This is further confirmed by the eight segment solution by Richmond[7] for a homogeneous medium (i.e., $d = \infty$).

Also presented in Fig. 11 is a comparison with a Sommerfeld integral solution by program WFLLL2B[8]. It is emphasized that with this program 21 segments were required to obtain the results presented, which is equivalent of 105 segments per wavelength in the earth. In comparison it is seen that good results are obtained for this antenna (which is 0.2λ long in the earth) by using only two segments and the ASM. It is noted also that with WFLLL2B and 21 segments there is still some difficulty in matching the result for a homogeneous medium with those for the interface. Although the reactances obtained by the two methods differ slightly, the results are consistent.

The behaviour of the impedance in Fig. 11 is consistent with that observed for a dipole approaching a medium of lower conductivity shown in Figs. 9 and 10. Note that results could not be computed for the dipole in air with the interface present. A moment method solution[7] using 8 segments in free space yielded a value of 1.69 - j1036 for the input impedance. Note that the effect of conductive earth contact is to greatly increase the input resistance. As noted before, the reactance change is primarily due to the change in the electrical length of the antenna as the interface is approached. The resistance is largely unaffected because of the power input to the antenna being absorbed by the earth.

The computation time is observed to vary approximately as d^{-1}. Consequently the results for small d are relatively time consuming. Table II shows the computer time required to calculate the results shown in Fig. 6 for two convergence accuracies. The computer used was a Datacraft 6024, but the times have been presented for an IBM 370/168 computer by running one example and converting all times by the speed ratio thus obtained.

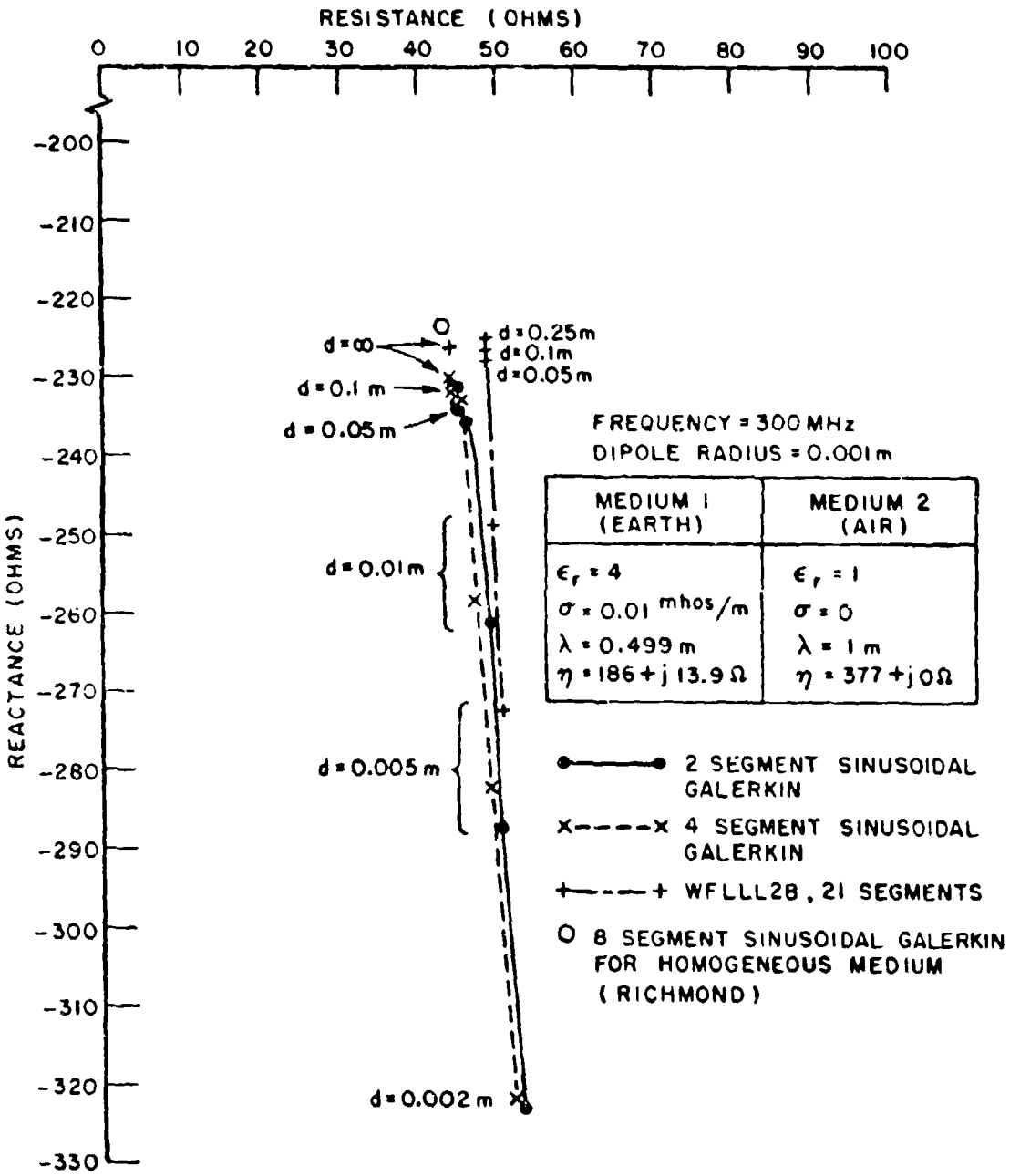

Fig. 11. Input impedance of 0.1m dipole buried in a lossy half space (earth).

TABLE II

IBM 370/168 COMPUTER TIME REQUIRED TO COMPUTE
THE RESULTS PRESENTED IN Fig. 6

distance from interface d	Seconds of CPU time for convergence = 10^{-3}	Seconds of CPU time for convergence = 10^{-4}
.5 m	.85	0.87
.25 m	1.05	1.23
.1 m	3.37	4.27
.05 m	8.41	12.4
.01 m	28.6	46.3
.005 m	45.6	103
.001 m	117	477

For d = .001 m, the impedance calculated with a convergence accuracy of 10^{-3} was 4.697 - j148.4Ω. When the convergence accuracy was increased to 10^{-4} the calculated impedance was 4.285 - j143.8Ω. It is doubtful if the improvement in accuracy justifies the large increase in computer time. Large amounts of computer time are required when d is less than about λ/1000.

In Table III a CPU time comparison is made between the ASM and the Sommerfeld program WFLLL2B[8]. Since the ASM is similar to a Sommerfeld approach[3] no dramatic differences in CPU time are observed. It is apparent however that far fewer segments are needed with the ASM because of the superiority of the piecewise sinusoidal current expansion for wire antennas. It should also be noted that the pilot subroutine used trapezoidal integration. A significant improvement is likely if a more efficient integration procedure is used.

It is also worth pointing out that our pilot subroutine which computes the values of the integrand contains only 65 FORTRAN statements. A further 13 statements are added to calculate r_{n_0,k_0}, and the integration subroutine contains 70 statements.

TABLE III

IBM 370/168 CPU TIME IN SECONDS REQUIRED TO COMPUTE THE RESULTS PRESENTED IN Fig. 11

d (meters)	Array scanning method		Program WF-LLL-2B 21 segments
	4 segments	2 segments	
.25 m	5.6	1.2	68
.1 m	17.5	4.2	59
.05 m	56.3	12.3	79
.01 m	341	45	105
.005 m	526	101	136

V. THE IMPEDANCE OF DIPOLES IN A CONDUCTING HALF-SPACE

Subterranean electromagnetic pulse radar systems for probing many hundreds of meters into the earth must necessarily operate at low frequencies[9]. Physically long antennas lying on the surface or buried only a few centimeters from the surface are required. This close electrical spacing to the surface threatens the viability of this method for calculating the input impedance of these antennas. Fortunately advantage can be taken of the low frequency characteristics of the earth.

At low frequencies where the earth is classed as a conductor ($\alpha = \beta$), the higher attenuation constant assists convergence (rate of convergence for large n_0 and k_0 in Eq. (1) depends upon the real part of γc_y, which varies in a rather complicated way with frequency and constitutive parameters). Further economies in computer time are possible at low frequencies by reducing the number of integration steps N. This is due to the increased attenuation between the array elements as the wavelength becomes large (which means that the array spacing, which we set at 0.5λ in our numerical calculations, becomes large).

In this section calculations of the input impedance of a 1000 m dipole in earth of constitutive parameters $\varepsilon_r = 4$, $\sigma = .01$ mhos/meter are presented for a frequency of 100 Hz. It was possible to calculate results with the antenna as close as 2 cm to the interface with reasonable expenditure of computer time (2 cm is about 1/150,000 of a wavelength in the earth). For this example good results were obtained when the dipole was within 0.1λ ($\approx$ 300m) of the interface by evaluating

only the integrand of Eq. (6) (i.e., N = 0) with $\sin\theta = \sin\phi = 0$. This means that the mutual impedance of the array is almost identical to the mutual impedance of a single element. This occurs because at 100 Hz the array is spaced $\lambda/2 = 1581$ meters between elements, and the high loss means that only the fields of the center element are significant providing the reference dipole is located near the center element.

Figure 12 plots the error in the mutual impedance of two parallel 1000m sinusoidal dipoles in an infinite medium of $\epsilon_r = 4$, $\sigma = .01$ mhos/meter when calculated using this approximation. The induced emf method was used as a reference. The error is seen to increase as the separation of the dipoles is reduced. The error also increases when the separation increases beyond 300m: this occurs because the spacing between the reference dipole and the adjacent-to-center elements of the array is less than an order of magnitude smaller than the spacing of the reference dipole and the center element. This error can be reduced by performing the integration in Eq. (6), i.e., N > 0. However the integration was observed to have little effect on the error at close spacings, supporting the assumption that the mutual impedance is dominated by the fields of the center element of the array. The computer time required is indicated on Fig. 12: the saving is seen to be roughly 50x by comparison with Table II for similar electrical spacings.

Using the array approximation, the input impedance of the 1000m dipole buried in the earth was calculated. The results are shown in Fig. 13. The convergence accuracy chosen was 0.5×10^{-3}. Since the induced emf method, which is used to calculate the self impedance, is assumed accurate, and Fig. 12 gives the expected accuracy of the mutual impedance of the image in the interface assuming perfect reflection, the overall accuracy of the calculations presented in Fig. 13 can be estimated. The error in the reactance is estimated to be less that 1% for all d, and the error in the input resistance is estimated to be less than 2% when d = 1m.

When d = 0.1m, the error in the resistance exceeds 8%. It is interesting to note that when d < 0.1m the error in the mutual impedance computations acts to make the mutual (and hence self) impedance constant. This effect was also noticed when preparing Fig. 12, hence it is not a property of the half-space (i.e., although the error increases as the spacing decreases, the mutual impedance calculated by the ASM is observed to become independent of spacing).

The economies in computer time (indicated by the CPU times included in Fig. 13) obtained by the array approximation described in this section make this technique useful for more accurate analysis of dipoles by the moment method. As an example, the input impedance of the 1000m dipole obtained from a four segment (equal lengths) moment method solution using sinusoidal bases and Galerkins method is presented in Fig. 14. Note the improvement in accuracy for small d, and the appearance of the "kink" near $d = \infty$, commonly observed in the lossy dielectric results. Results for a higher series convergence accuracy (10^{-4}) are given in Fig. 15. As concluded in the previous section, the improvement in accuracy does not warrant the large increase in computer time.

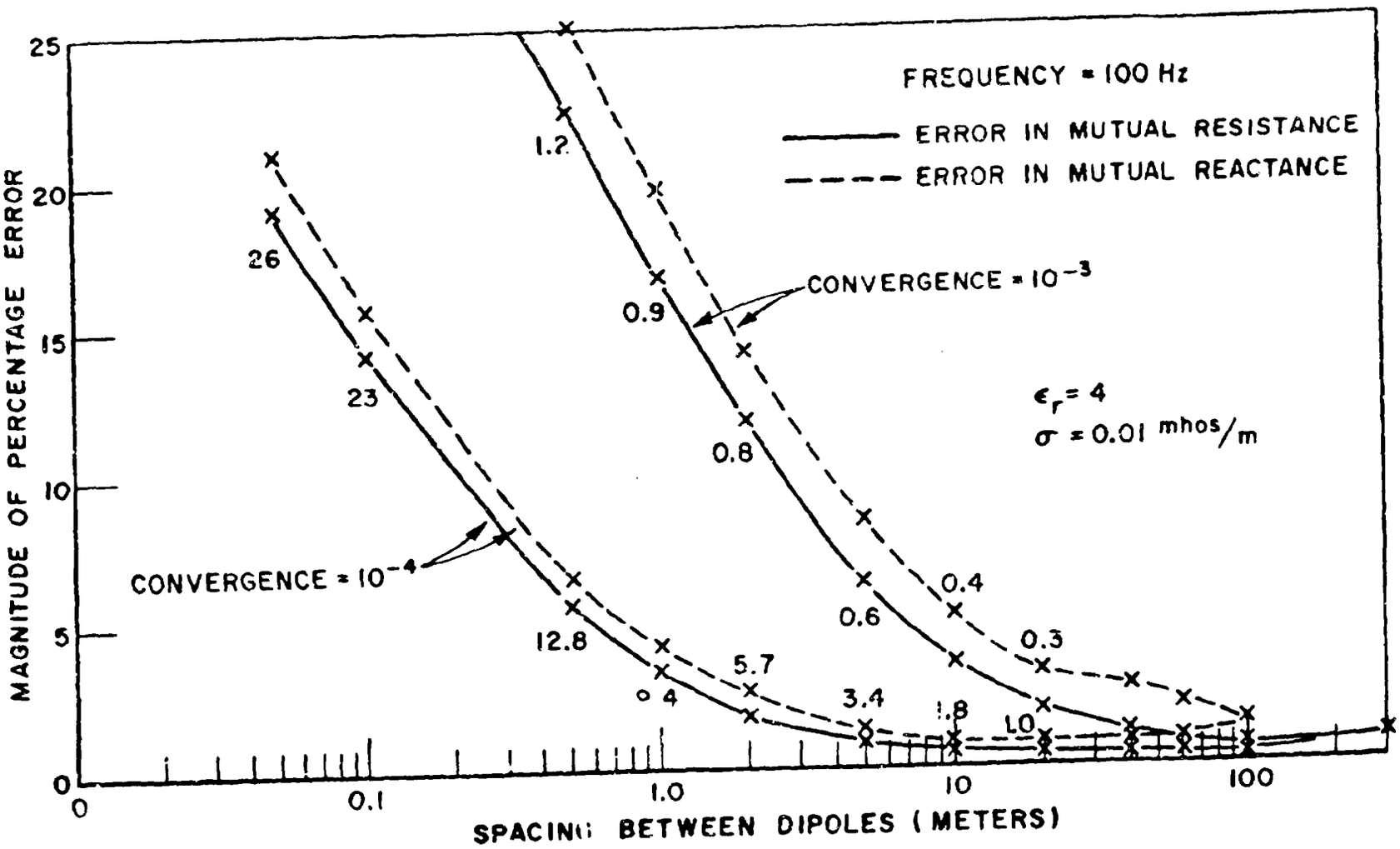

Fig. 12. Error in computing mutual impedance between 1000m parallel sinusoidal dipoles by array scanning method. The numbers beside the curves are the computing times in seconds on IBM 370/168 computer for the mutual impedance by the array scanning method.

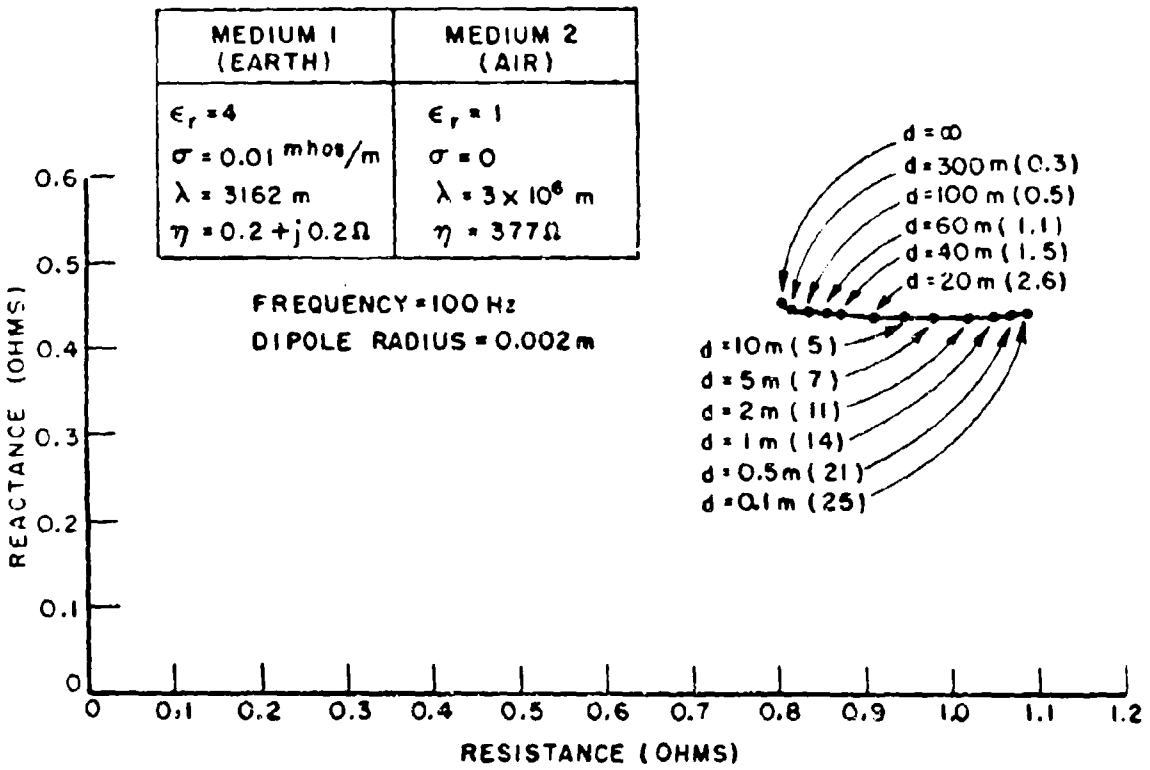

Fig. 13. Input impedance of 1000m long sinusoidal dipole buried in a conducting half space (earth). The computation times in seconds for an IBM 370/168 computer are given in parenthesis.

It is interesting to note from Fig. 15 that when the dipole approaches the air interface from the conducting medium that the only significant change occurs in the input resistance. The results presented indicate that if the dipole was brought from d = ∞ into close contact with the interface then the input resistance would approximately double. This confirms the simple physical argument: there is only one conducting half space to shunt the antenna so that the input resistance is doubled.

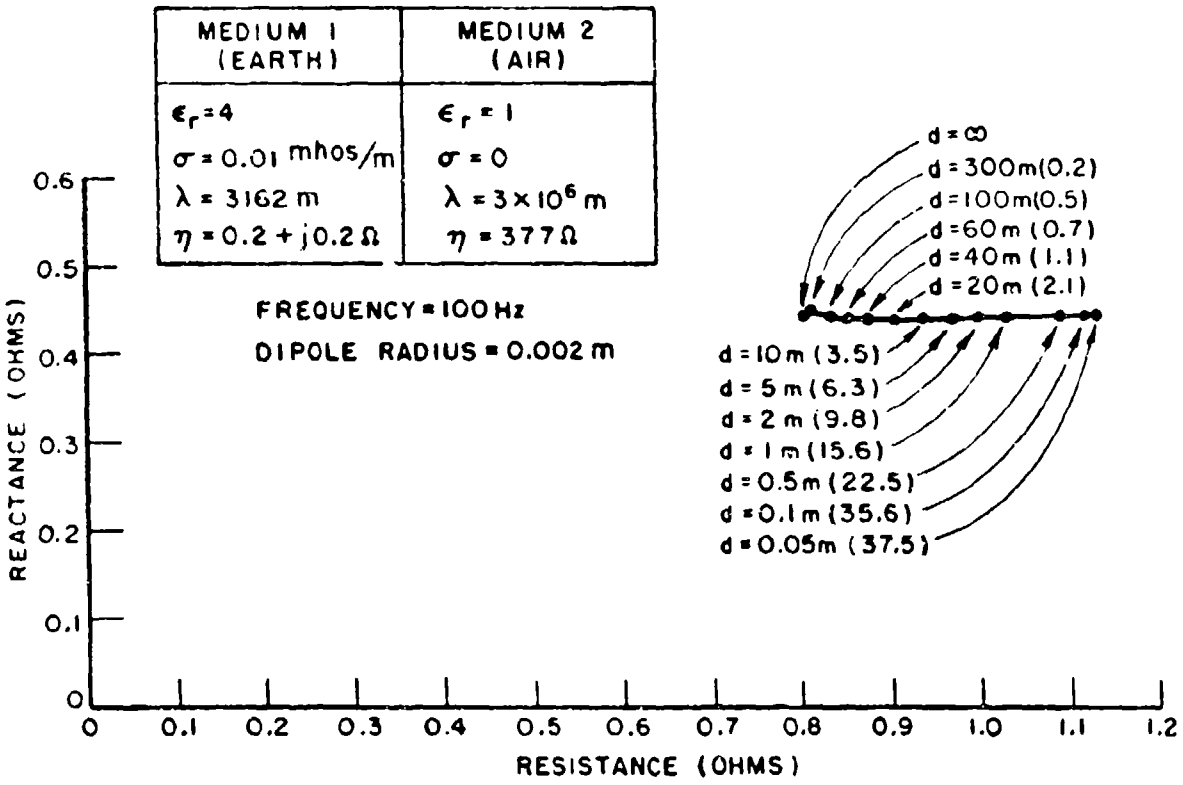

Fig. 14. Four segment sinusoidal Galerkin moment method solution for input impedance of 1000m long dipole buried in a conducting half-space (earth). The series convergence accuracy was 0.5×10^{-3}. IBM 370/168 computation times in seconds are given in parenthesis.

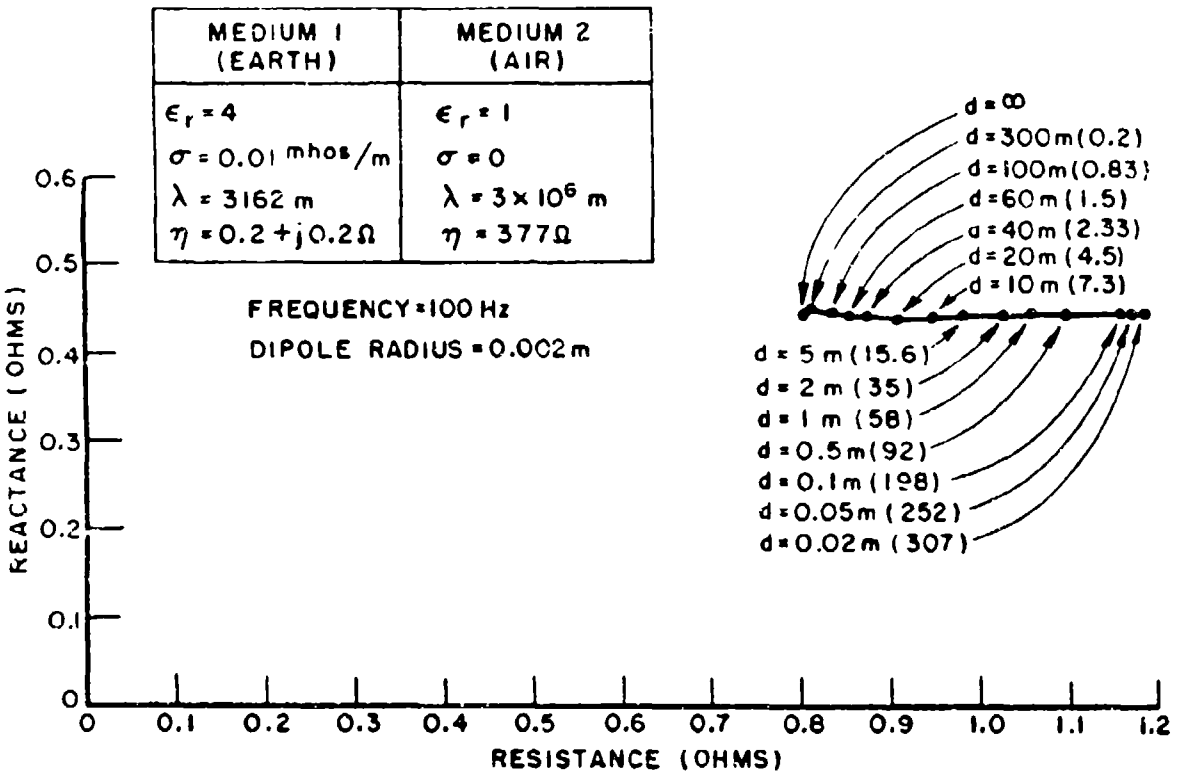

Fig. 15. Four segment sinusoidal Galerkin moment method solution for input impedance of 1000m long dipole buried in a conducting half space (earth). The series convergence accuracy was 10^{-4}. IBM 370/168 computation times in seconds are given in parenthesis.

Multisegment moment method solutions with small segments are more accurate than simple two segment solutions because the current distribution is more accurately represented. With a two segment solution it is assumed that the current distribution remains unchanged as the dipole approaches the interface. The accuracy of this assumption can be gauged from the four segment solution. Table IV shows the current relative to the terminal current at a point halfway between the center terminals and the dipole tip as the dipole aporoaches the interface. If the medium containing the dipole was lossless, the magnitude of the current would have been slightly greater than 0.5 (since the sinusoidal shape of the distribution begins to show when the antenna is 0.3λ long) and the phase near zero. The attenuation of the medium acts to reduce the magnitude of the current along the antenna, and causes the negative phase angle. The physical explanation is that the reflection of the input wave from the tips of the antenna is attenuated, and when summed with the outgoing wave results in a current amplitude with a negative phase angle. Notice in Table IV that as the antenna comes close to the surface the immediate environment of the antenna becomes less lossy, thereby reducing the phase and increasing the magnitude of the current at the midpoint of each side of the antenna.

TABLE IV

AMPLITUDE OF THE CURRENT RELATIVE TO THE TERMINAL CURRENT 250m FROM THE TERMINALS OF A CENTER FED 1000m DIPOLE IN CONDUCTING EARTH PARALLEL TO AN AIR INTERFACE

distance from interface d (metres)	Relative amplitude of current
300	0.470/-15.7°
100	0.46[illegible]/-15.6°
60	0.463/-15.5°
40	0.464/-15.3°
20	0.464/-14.6°
10	0.465/-13.9°
5	0.467/-13.3°
2	0.470/-12.4°
1	0.471/-11.9°
0.5	0.473/-11.4°
0.1	0.476/-10.6°
0.05	0.476/-10.4°
0.02	0.477/-10.3°

VI. CONCLUSIONS

A simple alternative formulation of the classical Sommerfeld problem called the Array Scanning Method (ASM) has been applied to linear sinusoidal antennas in a lossy half space. The advantage of the method are:

1. It is simple to program and the resulting program occupies significantly less storage than does a typical Sommerfeld program.

2. The formulation has a clear physical interpretation which greatly facilitates its use.

It is shown that at low frequencies, the input resistance of a dipole buried in the earth approximately doubles when it is moved from large depths to a position near the interface. This confirms the simple physical argument: there is only one conducting half-space to shunt the antenna so that the resistance is doubled.

Although the numerical evaluation of the integral is not as straightforward when the antenna is in free space, the method has been shown to converge in this case, and with a suitable integration procedure could be applied to the analysis of linear antennas above the earth.

REFERENCES

[1] A. Banos, Dipole Radiation in the Presence of a Conducting Half-Space, New York: Permagon Press, 1966.

[2] J.H. Richmond, "Radiation and Scattering by Thin-Wire Structures in the Complex Frequency Domain," National Aeronautics and Space Administration, NASA CR-2396, May 1974.

[3] B.A. Munk, R.D. Fulton and R.J. Luebbers, "Plane Wave Expansion for Arrays in Presence of Dielectric Slabs," Report AFAL-TR-76-53, prepared by the Ohio State University ElectroScience Laboratory for Air Force Avionics Laboratory, Wright-Patterson Air Force Base, Ohio.

[4] R.C. Hansen, Microwave Scanning Antennas, New York: Academic, 1966.

[5] E.C. Jordan and K.G. Balman, Electromagnetic Waves and Radiating Systems, second edition. New Jersey: Prentice Hall, 1966.

[6] D.L. Moffatt, R.J. Puskar and L. Peters, Jr., "Electromagnetic Pulse Sounding for Geological Surveying with Application in Rock Mechanics and the Rapid Excavation Program, Report 3208-2, September 1973, The Ohio State University ElectroScience Laboratory, Department of Electrical Engineering; prepared under Contract H0230009 for Bureau of Mines.

[7] J.H. Richmond, "Radiation and Scattering by Thin-Wire Structures in a Homogeneous Conducting Medium," IEEE Trans. Antennas Propagat., vol. AP-22, p. 365, March 1974.

[8] D.L. Lager and R. Jeff Lytle, "Fortran Subroutines for the Numerical Evaluation of Sommerfeld Integrals unter anderem," Report UCRL-51821, Lawrence Livermore Laboratory, University of California, Livermore.

[9] R. Gabillard, P. Degauque and J.R. Wait, "Subsurface Electromagnetic Telecommunication - A Review," IEEE Trans. Comm. Tech., vol. COM-19, pp. 1217-1228, December 1971.

APPENDIX A

MUTUAL IMPEDANCE OF PARALLEL SINUSOIDAL DIPOLES BY THE ARRAY SCANNING METHOD

Consider a reference dipole located parallel to an infinite plane array in a lossy medium with ε and σ, as shown in Fig. 1. The displacements from the x axis are X and Z. Following Munk, et al[3] the current on the element in the kth column and nth row of the array is given by

$$(11) \qquad I_{kn} = I\, e^{j\beta n D_x \sin\theta}\, e^{j\beta k D_z \sin\phi}$$

where $I = \sinh\gamma(\ell - |z|)/\sinh\gamma\ell$ is the current on the centre element, $\gamma = \alpha + j\beta$ is the propagation constant, and θ and ϕ are phase differences in the current on adjacent elements in the z direction and x direction respectively.

The mutual impedance between the reference dipole and the array Z_M^a can be obtained by summing the mutual impedances of each element of the array:

$$(12) \qquad Z_M^a = \sum_{k=-\infty}^{\infty} \sum_{n=-\infty}^{\infty} Z_{o,kn}\, e^{j\beta n D_x \sin\theta}\, e^{j\beta k D_z \sin\phi} \quad .$$

$Z_{o,kn}$ is the mutual impedance between the reference dipole and the knth element of the array, and is given by[5]

$$(13) \qquad Z_{o,kn} = \frac{-\eta}{4\pi \sinh^2\gamma\ell} \int_{-\ell}^{\ell} \left[\frac{e^{-\gamma r_1}}{r_1} + \frac{e^{-\gamma r_2}}{r_2} - 2\cosh\gamma\ell\, \frac{e^{-\gamma r_o}}{r_o} \right] \sinh\gamma(\ell - |z|)\, dz$$

where η is the characteristic impedance of the medium, and

$$(14) \qquad r_o^2 = (kD_x - X)^2 + d_1^2 + (nD_z - Z - z)^2$$

$$(15) \qquad r_1^2 = (kD_x - X)^2 + d_1^2 + (nD_z - Z - z + \ell)^2$$

$$(16) \qquad r_2^2 = (kD_x - X)^2 + d_1^2 + (nD_z - Z - z - \ell)^2$$

as shown in Fig. 16.

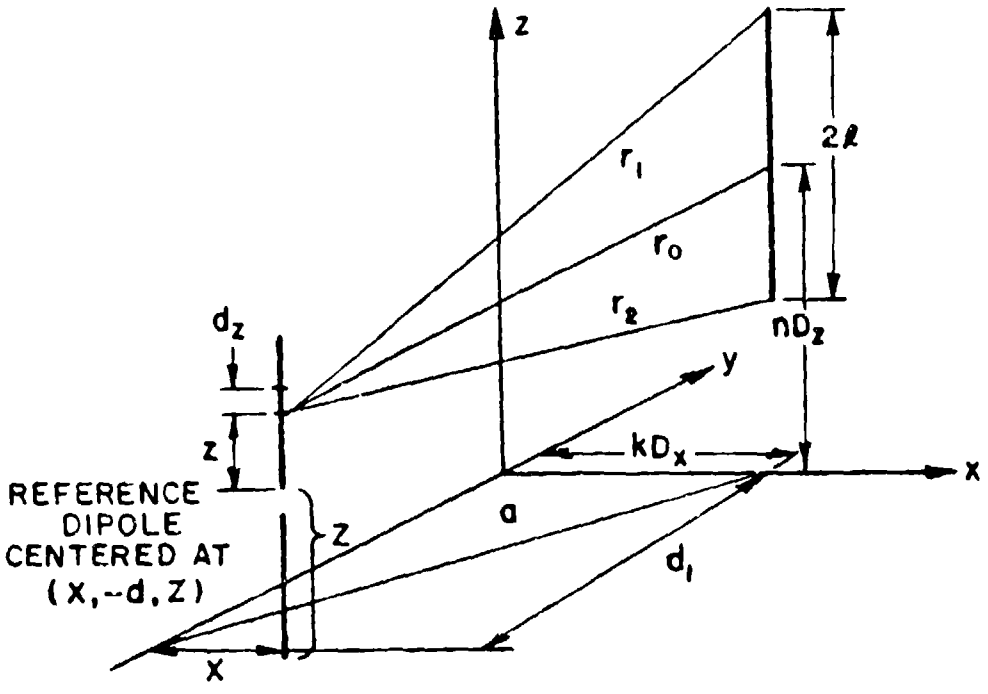

Fig. 16. The geometry involving the reference dipole at (X,-d,Z) and the kn'th dipole of the array.

Equation (12) can be written as

$$Z_M^a = \sum_{k=-\infty}^{\infty} Z_1 \, e^{j\beta k D_z \sin\phi} \tag{17}$$

where

$$Z_1 = \frac{-\eta}{4\pi \sinh^2 \gamma\ell} \sum_{n=-\infty}^{\infty} \int_{-\ell}^{\ell} \left[\frac{e^{-\gamma r_1}}{r_1} + \frac{e^{-\gamma r_2}}{r_2} - \frac{2e^{-\gamma r_o}}{r_o} \cosh\gamma\ell \right] e^{j\beta n D_z \sin\theta} \sinh\gamma(\ell - |z|)\,dz \tag{18}$$

Reversing the order of integration and summation in Eq. (18) gives

$$(19)\qquad Z_1 = \frac{-\eta}{4\pi \sinh^2 \gamma \ell} \int_{-\ell}^{\ell} \sinh\gamma(\ell-|z|) \sum_{n=-\infty}^{\infty} \left[\frac{e^{-\gamma r_1}}{r_1} + \frac{e^{-\gamma r_2}}{r_2} - 2\,\frac{e^{-\gamma r_o}}{r_o} \cosh\gamma\ell \right] e^{j\beta n D_z \sin\theta}\, dz \quad .$$

By combining the Poisson sum formula

$$(20)\qquad \sum_{n=-\infty}^{\infty} F(n\omega) e^{jn\omega t} = T \sum_{n_o=-\infty}^{\infty} f(t+n_o T) \; ; \qquad T = \frac{2\pi}{\omega_o}$$

and the frequency shift theorem

$$(21)\qquad F(\omega - W) \overset{\text{Fourier}}{\longleftrightarrow} f(t)\, e^{jWt}$$

where W is a radian frequency shift, we obtain

$$(22)\qquad \sum_{n=-\infty}^{\infty} F(\omega-W)\, e^{jn\omega t} = T \sum_{n_o=-\infty}^{\infty} e^{jW(t+n_o T)}\, f(t+n_o T) \quad .$$

The summation in Eq. (18) can be done by applying Eq. (22) with the Fourier Transform pair

$$(23)\qquad \frac{e^{-\gamma\sqrt{a^2+(\omega-\omega_1)^2}}}{\sqrt{a^2+(\omega-\omega_1)^2}} \overset{\text{Fourier}}{\longleftrightarrow} e^{j\omega_1 t} \cdot \frac{-j}{2}\, H_o^{(2)}\left(a\sqrt{-\gamma^2-t^2}\right)$$

and by making the following substitutions

$$(24)\qquad \omega = D_z$$

$$(25)\qquad t = \beta \sin\theta$$

$$(26)\qquad \omega_1 = \begin{cases} z-\ell & \text{for } r_1 \\ z & \text{for } r_o \\ z+\ell & \text{for } r_2 \end{cases}$$

(27) $$W = Z$$

(28) $$a^2 = (kD_x - X)^2 + d^2$$

(29) $$T = \frac{2\pi}{D_z} \quad .$$

Equation (18) then becomes

(30) $$Z_1 = \frac{-\eta}{2D_z \sinh^2 \gamma\ell} \int_{-\ell}^{\ell} \sinh\gamma(\ell - |z|) \sum_{n_0=-\infty}^{\infty} \left[e^{j\beta Z s_\theta} (2\cos\beta\ell s_\theta - 2\cosh\gamma\ell) \left(\frac{j}{2} H_0^{(2)} \left(a\sqrt{-\gamma^2 - \beta^2 s_\theta^2} \right) \right) \right]$$

where s_θ is defined in Eq. (5).

After doing the integration we get

(31) $$Z_1 = \frac{-j\eta}{D_z} \sum_{n_0=-\infty}^{\infty} P^2(\theta) e^{j\beta Z s_\theta} \left[H_0^{(2)} \left(a\sqrt{-\gamma^2 - \beta^2 s_\theta^2} \right) \right]$$

where $P^2(\theta)$ is defined in Eq. (3).

Z_1 is the mutual impedance between the reference dipole and an infinite column of dipoles spaced D_z metres apart in the z direction. The mutual impedance between the centre dipole only and the reference dipole can now be inferred from the column array impedance Eq. (31) by using the Fourier series for a periodic function:

(32) $$T \sum_{m=-\infty}^{\infty} g(t+mT) = \sum_{n=-\infty}^{\infty} G(n\omega)\, e^{jn\omega t}$$

(33) $$\text{where } G(n\omega) = \int_{-T/2}^{T/2} g(t)\, e^{jn\omega t}\, dt \quad .$$

Combining Eqs. (32), (33) and (22), and setting n=0, we obtain

(34) $$F(-W) = \int_{-T/2}^{T/2} \sum_{n_0=-\infty}^{\infty} e^{jW(t+n_0T)} f(t+n_0T)\, dt \quad .$$

Making the substitutions given in Eqs. (24) - (29), we obtain

$$(35) \qquad Z_{oo} = \int_{-\pi/\beta D_z}^{\pi/\beta D_z} Z_1 \, d(\sin\theta) \quad .$$

$Z_{o,o}$ is the mutual impedance between the reference dipole, and the centre element of the z oriented column of dipoles located at z=0. Consider Eq. (35) when the element spacing $D_z = \lambda/2$. The integration limits then correspond to $-\pi/2 \leq \theta \leq \pi/2$. Physically Eq. (35) means that the phase of the current on the elements adjacent to the centre element is varied by π radians, the next elements by 2π radians, and so on, so that when the integration is done their mean field is zero at the reference dipole. Thus all elements but the centre element are "phased out". A time-frequency analogy is that the d.c. term is the average value of the time signal.

By substituting Eq. (35) into the expression for the mutual impedance of the infinite array Eq. (12) we obtain the mutual impedance of the reference dipole and an infinite number of dipoles spaced along the x axis $Z_{o,ko}$

$$(36) \qquad Z_{o,ko} = \frac{-jn}{D_z} \sum_{k=-\infty}^{\infty} \int_{-\pi/\beta D_z}^{\pi/\beta D_z} \sum_{n_o=-\infty}^{\infty} P^2(\theta) \, e^{j\beta Z s_\theta}$$

$$H_o^{(2)}\left(a\sqrt{-\gamma^2-\beta^2 s_\theta^2}\right) \, d(\sin\theta) \cdot e^{j\beta k D_z \sin\phi} \quad .$$

Reverse the order of summation and integration to obtain

$$(37) \qquad Z_{o,ko} = \frac{-jn}{D_z} \int_{-\pi/\beta D_z}^{\pi/\beta D_z} \sum_{n_o=-\infty}^{\infty} P^2(\theta) \, e^{j\beta Z s_\theta} \sum_{k=-\infty}^{\infty} H_o^{(2)}\left(a\sqrt{-\gamma^2-\beta^2 s_\theta^2}\right)$$

$$e^{j\beta k D_z \sin\phi} \, d(\sin\theta) \quad .$$

The k summation can be summed by again using Eq. (22) with the Fourier transform pair

$$(38) \qquad \frac{e^{-jd\sqrt{[-\gamma^2-\beta^2 s_\theta^2]-t^2}}}{\pi\sqrt{[-\gamma^2-\beta^2 s_\theta^2]-t^2}} \quad \text{Fourier} \longleftrightarrow \quad H_o^{(2)}\left(\sqrt{[-\gamma^2-\beta^2 s_\theta^2]}\,\sqrt{\omega^2+d^2}\right) \quad .$$

The necessary substitutions are

(39) $$T = \frac{2\pi}{D_x}$$

(40) $$t = \beta \sin\phi$$

(41) $$\omega = D_x$$

(42) $$W = X,$$

so that

(43) $$Z_{o,ko} = \frac{-j2\eta}{D_x D_z} \int_{-\pi/\beta D_z}^{\pi/\beta D_z} \sum_{n_o=-\infty}^{\infty} p^2(\theta) e^{j\beta Z s_\theta} \sum_{k_o=-\infty}^{\infty} e^{j\beta X s_\phi} \frac{e^{-jd\sqrt{-\gamma^2-\beta^2(s_\theta^2+s_\phi^2)}}}{\sqrt{-\gamma^2-\beta^2(s_\theta^2+s_\phi^2)}} \cdot d(\sin\theta)$$

where s_ϕ is given in Eq. (5).

By again applying Eq. (34) with Eqs. (39) - (42) we eliminate all but the centre element. The result is

(44) $$Z_{o,oo} = \int_{-\pi/\beta D_z}^{\pi/\beta D_z} \int_{-\pi/\beta D_x}^{\pi/\beta D_x} Z_M \, d(\sin\phi) d(\sin\theta)$$

where

(45) $$Z_M = \frac{-j2\eta}{D_x D_z} \sum_{n_o=-\infty}^{\infty} p^2(\theta) e^{j\beta Z s_\theta} \sum_{k_o=-\infty}^{\infty} e^{j\beta X s_\phi} \frac{e^{-jd\sqrt{-\gamma^2-\beta^2(s_\theta^2+s_\phi^2)}}}{\sqrt{-\gamma^2-\beta^2(s_\theta^2+s_\phi^2)}} .$$

Equation (45) is the mutual impedance between the reference dipole and an infinite array, and Eq. (44) shows how the mutual impedance of a single element can be inferred from the array impedance by phasing out all elements but the centre element.

The important feature of Eq. (45) is that it contains a sum of plane waves. Recognizing this it can be written as

$$(46) \qquad Z_M = \frac{2\eta}{D_x D_z} \sum_{n_o=-\infty}^{\infty} P^2(\theta) e^{j\beta Z s_\theta} \sum_{k_o=-\infty}^{\infty} e^{j\beta X s_\phi} \frac{e^{-\gamma d c_y}}{\gamma c_y}$$

where the direction cosine c_y for the plane waves emitted by the array is defined in Eq. (2).

To obtain Eq. (46) it was necessary to use $\sqrt{-1} = -j$ so that the waves emitted by the array attenuate as they propagate away from the array. In Eq. (2) the required root is the principal root. The other direction cosines are

$$(47) \qquad c_x = \frac{j\beta s_\phi}{\gamma}$$

$$(48) \qquad c_z = \frac{j\beta s_\theta}{\gamma} \quad .$$